

## 24 V to 220 V Precision Operational Amplifier

### FEATURES

- ▶ Wide range of operating voltages
  - ▶ Dual-supply:  $\pm 12$  V to  $\pm 110$  V
  - ▶ Asymmetrical supply operation: 24 V to 220 V
- ▶ Wide input common-mode voltage range: 3 V from rails
- ▶ High common-mode rejection ratio: 160 dB typical
- ▶ High  $A_{OL}$ : 170 dB typical
- ▶ High slew rate
  - ▶ 74 V/ $\mu$ s typical
  - ▶ 24 V/ $\mu$ s typical with external input clamping diodes
- ▶ Low input bias current: 2 pA maximum
- ▶ Low input offset voltage: 1 mV maximum
- ▶ Low input offset voltage drift: 2  $\mu$ V/ $^{\circ}$ C maximum
- ▶ Low input voltage noise: 8 nV/ $\sqrt{\text{Hz}}$  typical at 10 kHz
- ▶ Wide small signal bandwidth: 10 MHz typical
- ▶ Resistor adjustable quiescent current: 0.6 mA to 3 mA ( $V_S = \pm 110$  V)
- ▶ Unity-gain stable
- ▶ Thermal monitoring
- ▶ Small footprint: 12-lead, 7 mm  $\times$  7 mm LFCSP compliant with IEC 61010-1 spacing
- ▶ Shutdown mode

### APPLICATIONS

- ▶ High-side current sensing
- ▶ Automated test equipment
- ▶ High voltage drivers
- ▶ Piezotransducers
- ▶ Digital-to-analog converter (DAC) output buffers
- ▶ Light detecting and ranging (LiDAR), avalanche photodiode (APD), single photon avalanche diode (SPAD) biasing

### TYPICAL APPLICATION CIRCUIT

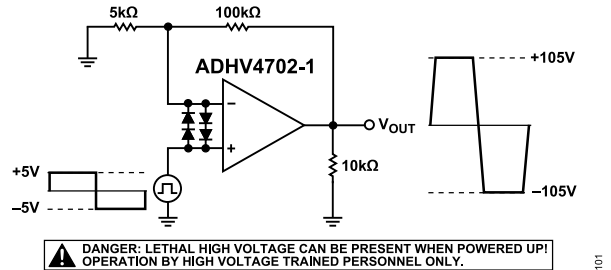


Figure 1.

### GENERAL DESCRIPTION

The ADHV4702-1 is a high voltage (220 V), unity-gain stable precision operational amplifier. The ADHV4702-1 offers high input impedance with low input bias current, low input offset voltage, low drift, and low noise for precision demanding applications. The next generation of proprietary semiconductor processes and innovative architecture from Analog Devices, Inc., enable this precision operational amplifier to operate from symmetrical dual supplies of  $\pm 110$  V, asymmetrical dual supplies, or a single supply of 220 V.

For precision performance, the ADHV4702-1 has a 170 dB typical open-loop gain ( $A_{OL}$ ) and a 160 dB typical common-mode rejection ratio (CMRR), as shown in Figure 3. The ADHV4702-1 also has a 2  $\mu$ V/ $^{\circ}$ C maximum input offset voltage ( $V_{OS}$ ) drift and an 8 nV/ $\sqrt{\text{Hz}}$  input voltage noise.

The exceptional dc precision of the ADHV4702-1 is complemented by excellent dynamic performance with a small signal bandwidth of 10 MHz and a slew rate of 74 V/ $\mu$ s. The ADHV4702-1 has an output current of 20 mA typical.

The ADHV4702-1 offers high voltage input common-mode swing as well as high voltage output swing, enabling precision high voltage use cases such as high-side current sensing.

The ADHV4702-1 is available in a **12-lead, 7 mm  $\times$  7 mm lead frame chip scale package (LFCSP)** with an exposed pad (EPAD) compliant to international electrotechnical commission (IEC) 61010-1 creepage and clearance standards. The copper EPAD provides a low thermal resistance path to improve heat dissipation and features high voltage isolation, allowing it to be safely connected to a 0 V ground plane regardless of VCC or VEE voltages. The ADHV4702-1 operates over the  $-40^{\circ}\text{C}$  to  $+85^{\circ}\text{C}$  industrial temperature range.

## TABLE OF CONTENTS

Features.....	1	Shutdown Pin ( $\overline{SD}$ ).....	16
Applications.....	1	Temperature Monitor (TMP).....	17
Typical Application Circuit.....	1	Overtemperature Protection.....	17
General Description.....	1	Output Current Drive and Short-Circuit Protection.....	17
Specifications.....	3	External Compensation and Capacitive Load ( $C_{LOAD}$ ) Driving.....	17
$\pm 12$ V to $\pm 110$ V Supply.....	3	Safe Operating Area.....	18
Absolute Maximum Ratings.....	5	LFCSP Package and High Voltage Pin Spacing.....	19
Maximum Power Dissipation.....	5	Exposed Pad (EPAD).....	19
Thermal Resistance.....	5	Applications Information.....	20
Electrostatic Discharge (ESD) Ratings.....	5	Power Supply and Decoupling.....	20
ESD Caution.....	5	High Voltage Guard Ring.....	20
Pin Configuration and Function Descriptions.....	6	High Voltage DAC Voltage Subtractor.....	20
Typical Performance Characteristics.....	7	High Current Output Driver.....	20
Theory of Operation.....	14	Signal Range Extender.....	20
Internal Electrostatic Discharge (ESD) Protection.....	14	Outline Dimensions.....	21
Slew Boost Circuit and Protection.....	14	Ordering Guide.....	21
Digital Ground (DGND).....	16	Evaluation Boards.....	21
Resistor Adjustable Quiescent Current (RADJ).....	16		

## REVISION HISTORY

**1/2023—Rev. B to Rev. C**

Changes to General Description Section.....	1
Changes to Figure 1.....	1
Added Electrostatic Discharge (ESD) Ratings Section.....	5
Added ESD Ratings for ADHV4702-1 Section and Table 4; Renumbered Sequentially.....	5
Moved Figure 3.....	7
Moved Figure 44.....	14
Changes to Figure 44.....	14
Changes to Figure 46.....	15
Changes to Figure 63.....	20
Changes to Figure 64.....	20
Changes to Figure 65.....	20

## SPECIFICATIONS

**±12 V TO ±110 V SUPPLY**

Supply voltage ( $V_S$ ) = ±12 V to ±110 V,  $T_A$  = 25°C with an EPAD connected to a 0 V analog ground (AGND), DGND pin tied to 0 V AGND,  $R_{ADJ}$  = 0  $\Omega$  ( $R_{ADJ}$  is a resistor that connects the RADJ pin to DGND), gain ( $A_V$ ) = 1, feedback resistor ( $R_F$ ) = 100 k $\Omega$ , and load resistance ( $R_{LOAD}$ ) = 10 k $\Omega$ , unless otherwise noted.

Table 1.

Parameter	Test Conditions/Comments	Min	Typ	Max	Unit
<b>DYNAMIC PERFORMANCE</b>					
-3 dB Bandwidth	$A_V = 1$ , output voltage ( $V_{OUT}$ ) = 200 mV p-p, $R_F = 0 \Omega$		10		MHz
Slew Rate	$A_V = 20$ , $V_{OUT} = 200$ V p-p, 20% to 80%		74		V/ $\mu$ s
	$A_V = 20$ , $V_{OUT} = 200$ V p-p, 20% to 80%, with external input clamping diodes <sup>1</sup>		24		V/ $\mu$ s
Settling Time to 0.1%	$A_V = 1$ , $V_{OUT} = 40$ V p-p, $R_F = 0 \Omega$		8.4		$\mu$ s
	$A_V = 20$ , $V_{OUT} = 40$ V p-p		6.2		$\mu$ s
	$A_V = 40$ , $V_{OUT} = 40$ V p-p		13		$\mu$ s
<b>NOISE PERFORMANCE</b>					
Input Voltage Noise	Frequency = 10 kHz		8		nV/ $\sqrt{\text{Hz}}$
Input Voltage Noise 1/f Corner			10		Hz
Input Current Noise	Frequency = 40 Hz		1		fA/ $\sqrt{\text{Hz}}$
<b>DC PERFORMANCE</b>					
Input Offset Voltage		-1	±0.15	+1	mV
Drift	$V_S = \pm 110$ V, $T_A = 25^\circ\text{C}$ to $85^\circ\text{C}$	-2	±0.25	+2	$\mu\text{V}/^\circ\text{C}$
	$V_S = \pm 12$ V, $T_A = 25^\circ\text{C}$ to $85^\circ\text{C}$	-3	±0.25	+3	$\mu\text{V}/^\circ\text{C}$
Input Bias Current	$T_A = 25^\circ\text{C}$	-2	±0.3	+2	pA
	$T_A = 85^\circ\text{C}$	-100	±19	+100	pA
Drift	$T_A = 25^\circ\text{C}$ to $85^\circ\text{C}$		±0.3		pA/ $^\circ\text{C}$
Input Offset Current	$T_A = 25^\circ\text{C}$	-2	±0.15	+2	pA
	$T_A = 85^\circ\text{C}$	-50	±8	+50	pA
Drift	$T_A = 25^\circ\text{C}$ to $85^\circ\text{C}$		±0.13		pA/ $^\circ\text{C}$
Open-Loop Gain	$V_S = \pm 110$ V	146	170		dB
	$V_S = \pm 12$ V	130	150		dB
<b>INPUT CHARACTERISTICS</b>					
Input Resistance					
Common-Mode	Common-mode voltage ( $V_{CM}$ ) = -60 V to +60 V		45		T $\Omega$
	$V_{CM} = -90$ V to +90 V		30		T $\Omega$
Differential			4.2		T $\Omega$
Input Capacitance					
Common-Mode			7.9		pF
Differential			17.9		pF
Input Common-Mode Voltage Range			±107		V
CMRR	$V_{CM} = -70$ V to +70 V	140	160		dB
<b>SHUTDOWN PIN (<math>\overline{\text{SD}}</math>)</b>					
$\overline{\text{SD}}$ Input Voltage					
Low	Disabled			0.8	V
High	Enabled	1.6			V
$\overline{\text{SD}}$ Input Current					
Low	$\overline{\text{SD}} = 0$ V		-11		$\mu\text{A}$
High	$\overline{\text{SD}} = 5$ V		-1		$\mu\text{A}$

## SPECIFICATIONS

Table 1. (Continued)

Parameter	Test Conditions/Comments	Min	Typ	Max	Unit
<b>OUTPUT CHARACTERISTICS</b>					
Output Voltage Range	$R_{LOAD} = 5\text{ k}\Omega$ , $T_A = -40^\circ\text{C}$ to $+85^\circ\text{C}$	108	108.5	-108	V
High					
Low					
Output Current			20		mA
<b>THERMAL MONITOR</b>					
TMP Pin Voltage <sup>2</sup>	$T_A = 25^\circ\text{C}$		1.9		V
TMP Pin Voltage Drift	$T_A = -40^\circ\text{C}$ to $+85^\circ\text{C}$		-4.5		mV/°C
<b>POWER SUPPLY</b>					
Operating Range	Symmetrical and asymmetrical supplies	24		220	V
Quiescent Current					
$\overline{SD} = 5\text{ V}$ (Enabled) <sup>3</sup>	$R_{ADJ} = 0\ \Omega$ , $T_A = 25^\circ\text{C}$ , $V_S = \pm 110\text{ V}$		3	3.3	mA
	$R_{ADJ} = 0\ \Omega$ , $T_A = 25^\circ\text{C}$ , $V_S = \pm 12\text{ V}$		2.7	3.3	mA
	$R_{ADJ} = 0\ \Omega$ , $T_A = -40^\circ\text{C}$ to $+85^\circ\text{C}$			3.3	mA
	$R_{ADJ} = 50\text{ k}\Omega$ , $T_A = 25^\circ\text{C}$ , $V_S = \pm 110\text{ V}$		0.9	1	mA
	$R_{ADJ} = 50\text{ k}\Omega$ , $T_A = 25^\circ\text{C}$ , $V_S = \pm 12\text{ V}$		0.8	1	mA
	$R_{ADJ} = 50\text{ k}\Omega$ , $T_A = -40^\circ\text{C}$ to $+85^\circ\text{C}$			1	mA
	$R_{ADJ} = 100\text{ k}\Omega$ , $T_A = 25^\circ\text{C}$ , $V_S = \pm 110\text{ V}$		0.6		mA
$\overline{SD} = 0\text{ V}$ (Disabled)			0.18	0.2	mA
Positive Power Supply Rejection Ratio (PSRR)	Positive supply voltage ( $+V_S$ ) = 107 V to 112.5 V, negative supply voltage ( $-V_S$ ) = 110 V	130	155		dB
	$+V_S = 10\text{ V}$ to $14\text{ V}$ , $-V_S = -12\text{ V}$	110	130		dB
Negative Power Supply Rejection Ratio	$+V_S = 110\text{ V}$ , $-V_S = -107\text{ V}$ to $-112.5\text{ V}$	130	155		dB
	$+V_S = 12\text{ V}$ , $-V_S = -10\text{ V}$ to $-14\text{ V}$	110	130		dB

<sup>1</sup> This slew rate result is tested while the ADHV4702-1 inputs are clamped at the forward-biased voltage of two diodes using ON Semiconductor® SBAV199LT1G. For more information, see the [Slew Boost Circuit and Protection](#) section.

<sup>2</sup> The TMP pin voltage may have device to device variation. For more information, see the [Temperature Monitor \(TMP\)](#) section.

<sup>3</sup> This specification is for quiescent current only. For supply current or dynamic supply current information, see the [Theory of Operation](#) section.

## ABSOLUTE MAXIMUM RATINGS

**Table 2.**

Parameter	Rating
Supply Voltage (VCC to VEE)	225 V
Output Voltage	VCC to VEE
Common-Mode Input Voltage	VCC to VEE
Differential Input Voltage	±2.0 V
Input Current	±5 mA
DGND Voltage	VCC - 12 V to VEE
Voltage	
RESERVED, $\overline{SD}$ , and TMP Pins	DGND to DGND + 6 V
COMP Pin	VCC - 5 V to VCC
RADJ Pin	DGND to DGND + 0.6 V
Storage Temperature Range	-65°C to +150°C
Operating Temperature Range	-40°C to +85°C
Lead Temperature (Soldering 10 sec) <sup>1</sup>	260°C
Junction Temperature (T <sub>J</sub> )	150°C

<sup>1</sup> See IPC/JEDEC J-STD-020 for more information.

Stresses at or above those listed under Absolute Maximum Ratings may cause permanent damage to the product. This is a stress rating only; functional operation of the product at these or any other conditions above those indicated in the operational section of this specification is not implied. Operation beyond the maximum operating conditions for extended periods may affect product reliability.

### MAXIMUM POWER DISSIPATION

The maximum safe power dissipation in the package is limited by the associated rise in T<sub>J</sub> on the die. At approximately 150°C, which is the glass transition temperature, the plastic begins to change its properties. Exceeding a T<sub>J</sub> of 150°C can result in changes in the silicon devices, potentially causing failure. [Table 3](#) shows the junction-to-case thermal resistance ( $\theta_{JC}$ ) for the LFCSP. For more detailed information on power dissipation and thermal management, see the [Applications Information](#) section.

### THERMAL RESISTANCE

Thermal performance is directly linked to printed circuit board (PCB) design and operating environment. Careful attention to PCB thermal design is required.

$\theta_{JA}$  is the natural convection, junction to ambient thermal resistance measured in a one cubic foot sealed enclosure.  $\theta_{JC}$  is the junction to case thermal resistance.

**Table 3. Thermal Resistance**

Package Type	$\theta_{JA}$	$\theta_{JC}$	Unit
CP-12-8 <sup>1</sup>	37	1	°C/W

<sup>1</sup> The data is collected from a 2S2P board. A cold plate is attached to the bottom side of the PCB using 100  $\mu$ m thermal interface material (TIM) for  $\theta_{JC}$  simulation. See JEDEC standard for additional information.

## ELECTROSTATIC DISCHARGE (ESD) RATINGS

The following ESD information is provided for handling of ESD-sensitive devices in an ESD protected area only.

Human body model (HBM) per ANSI/ESDA/JEDEC JS-001.

Field induced charged device model (FICDM) and charged device model (CDM) per ANSI/ESDA/JEDEC JS-002.

Machine model (MM) per ANSI/ESD STM5.2. MM voltage values are for characterization only.

### ESD Ratings for ADHV4702-1

**Table 4. ADHV4702-1, 12-Lead LFCSP**

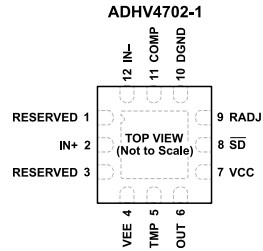
ESD Model	Withstand Threshold (V)	Class
FICDM	±750	C3
HBM	±1000	1C
MM	±100	A

### ESD CAUTION



**ESD (electrostatic discharge) sensitive device.** Charged devices and circuit boards can discharge without detection. Although this product features patented or proprietary protection circuitry, damage may occur on devices subjected to high energy ESD. Therefore, proper ESD precautions should be taken to avoid performance degradation or loss of functionality.

## PIN CONFIGURATION AND FUNCTION DESCRIPTIONS



NOTES  
 1. RESERVED, THESE PINS ARE INTERNALLY CONNECTED. FLOAT OR TIE THESE PINS TO THE DIGITAL GROUND.  
 2. EXPOSED THERMAL PAD. NO INTERNAL ELECTRICAL CONNECTION. TIE EPAD TO EXTERNAL GROUND PLANE AND/OR HEAT SINK FOR THERMAL MANAGEMENT.

Figure 2. Pin Configuration

Table 5. Pin Function Descriptions

Pin No.	Mnemonic	Description
1, 3	RESERVED	Reserved. These pins are internally connected. Float or connect these pins to the digital ground.
2	IN+	Noninverting Input.
4	VEE	Negative Power Supply Input.
5	TMP	Temperature Monitor Output.
6	OUT	Output.
7	VCC	Positive Power Supply Input.
8	$\overline{SD}$	Shutdown (Active Low). $\overline{SD}$ is referenced to DGND.
9	RADJ	Resistor Adjustable Quiescent Current. Connect RADJ to DGND to fully bias the amplifier.
10	DGND	Logic Reference for RADJ and $\overline{SD}$ . Connect DGND to 0 V analog ground.
11	COMP	External Compensation.
12	IN-	Inverting Input.
	EPAD	Exposed Thermal Pad. No internal electrical connection. Tie EPAD to external ground plane and/or heat sink for thermal management.

TYPICAL PERFORMANCE CHARACTERISTICS

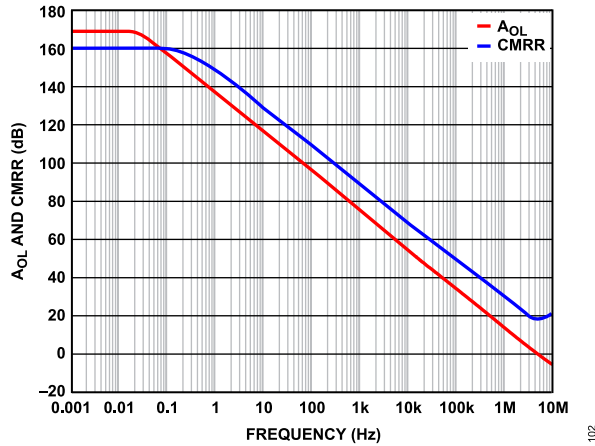


Figure 3. ADHV4702-1 Precision Performance

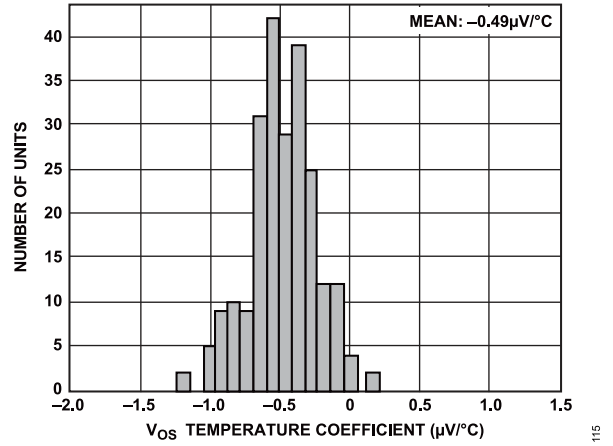


Figure 6. Input Offset Voltage Drift Distribution,  $T_A = 25^\circ\text{C}$ ,  $V_S = \pm 110\text{V}$ ,  $V_{CM} = 0\text{V}$ ,  $\Delta T_J = 60^\circ\text{C}$ ,  $R_{ADJ} = 0\ \Omega$

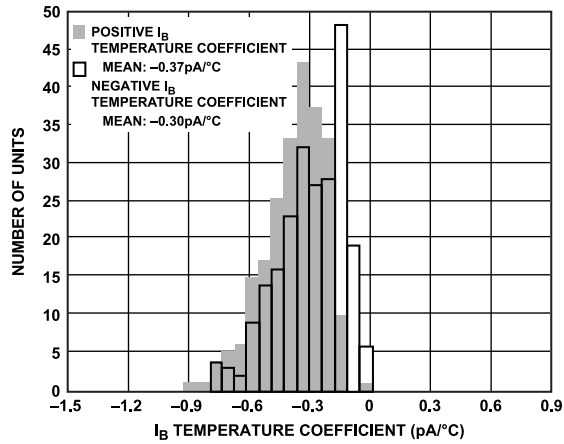


Figure 4. Positive and Negative Input Bias ( $I_B$ ) Current Drift Distribution,  $T_A = 25^\circ\text{C}$ ,  $V_S = \pm 110\text{V}$ ,  $V_{CM} = 0\text{V}$ ,  $\Delta T_A = 60^\circ\text{C}$ ,  $R_{ADJ} = 0\ \Omega$

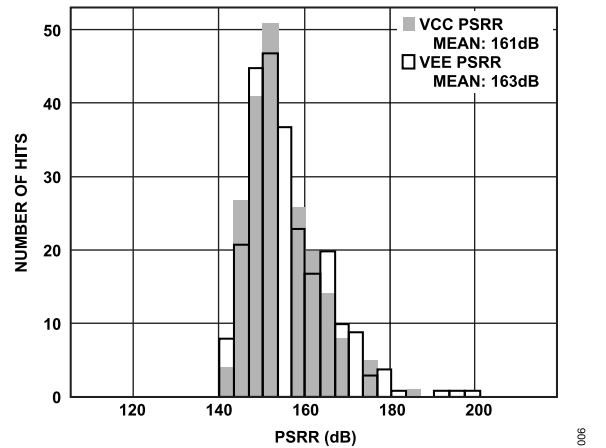


Figure 7. PSRR Distribution,  $T_A = 25^\circ\text{C}$ ,  $V_S = \pm 110\text{V}$ ,  $R_{ADJ} = 0\ \Omega$

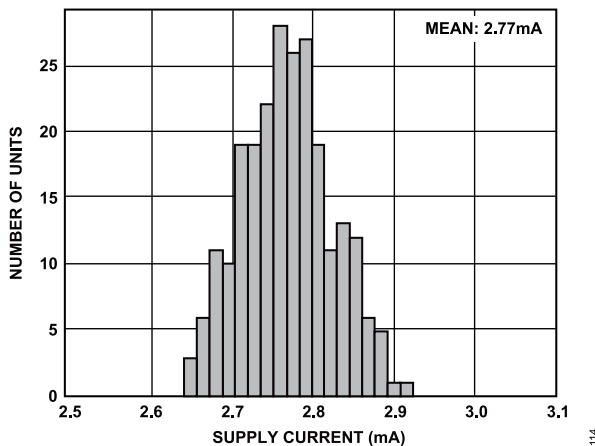


Figure 5. Supply Current Distribution,  $T_A = 25^\circ\text{C}$ ,  $V_S = \pm 110\text{V}$ ,  $R_{ADJ} = 0\ \Omega$

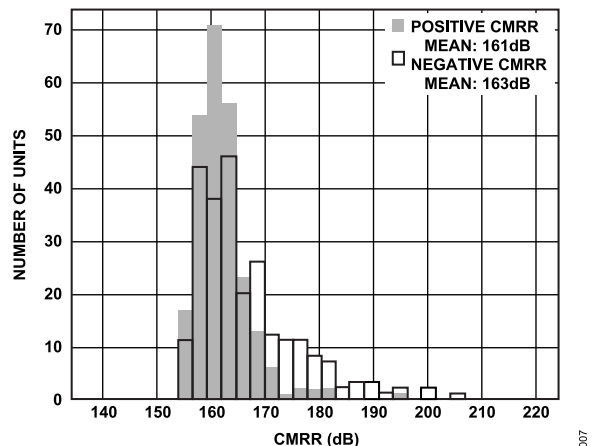


Figure 8. CMRR Distribution,  $T_A = 25^\circ\text{C}$ ,  $V_S = \pm 110\text{V}$ ,  $R_{ADJ} = 0\ \Omega$

TYPICAL PERFORMANCE CHARACTERISTICS

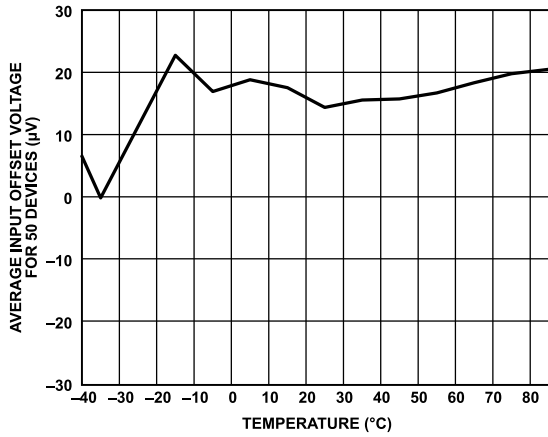


Figure 9. Average Input Offset Voltage for 50 Devices vs. Temperature,  $V_S = \pm 110\text{ V}$

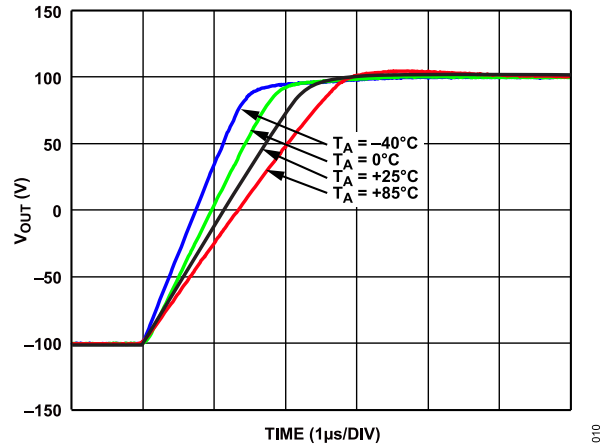


Figure 12. Large Signal Pulse Response at Various  $T_A$ , Rising Edge,  $A_V = 20$ ,  $V_S = \pm 110\text{ V}$ ,  $V_{OUT} = 200\text{ V p-p}$ ,  $R_F = 100\text{ k}\Omega$ ,  $R_{LOAD} = 10\text{ k}\Omega$ ,  $R_{ADJ} = 0\ \Omega$

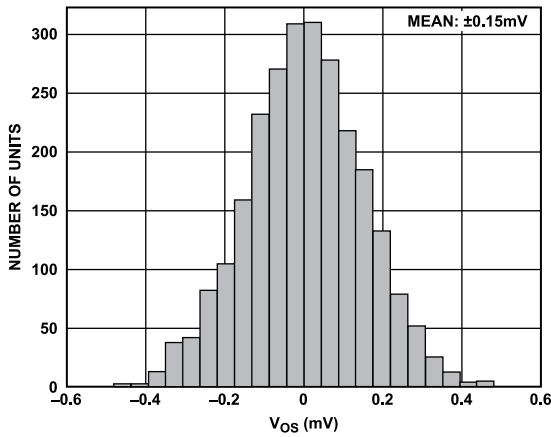


Figure 10. Input Offset Voltage Distribution,  $T_A = 25^\circ\text{C}$ ,  $V_S = \pm 110\text{ V}$ ,  $V_{CM} = 0\text{ V}$ ,  $R_{ADJ} = 0\ \Omega$

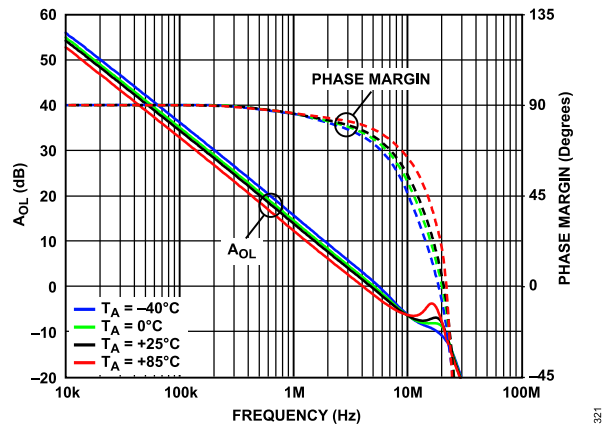


Figure 13.  $A_{OL}$  and Phase Margin vs. Frequency at Various  $T_A$ ,  $V_S = \pm 110\text{ V}$ ,  $R_{ADJ} = 0\ \Omega$

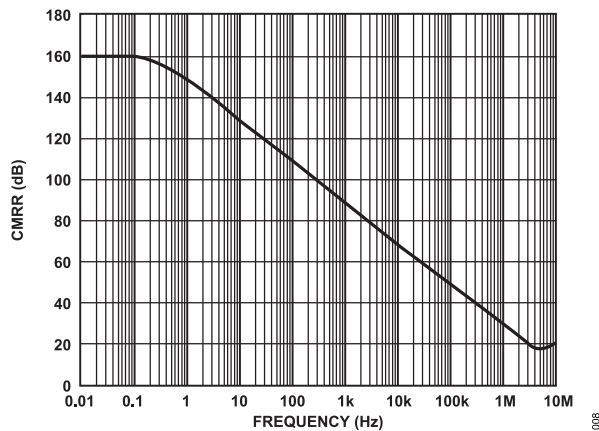


Figure 11. CMRR vs. Frequency,  $T_A = 25^\circ\text{C}$ ,  $V_S = \pm 110\text{ V}$ ,  $R_{LOAD} = 10\text{ k}\Omega$ ,  $R_{ADJ} = 0\ \Omega$

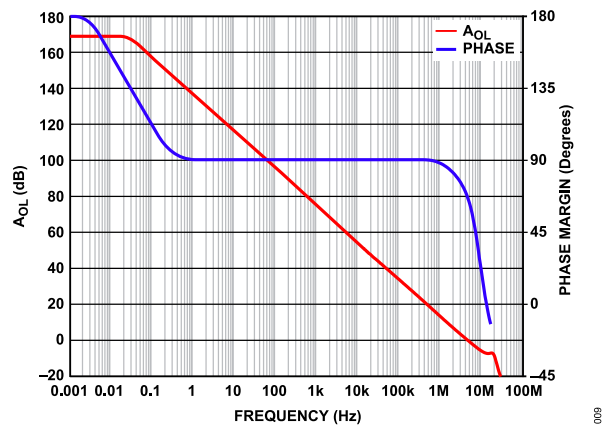


Figure 14.  $A_{OL}$  and Phase Margin vs. Frequency,  $T_A = 25^\circ\text{C}$ ,  $V_S = \pm 110\text{ V}$ ,  $R_{ADJ} = 0\ \Omega$



TYPICAL PERFORMANCE CHARACTERISTICS

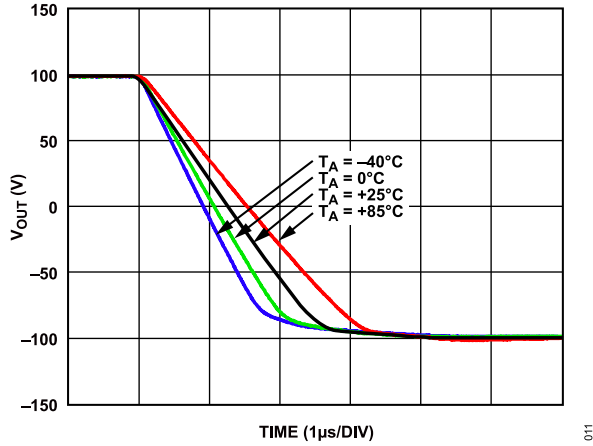


Figure 15. Large Signal Pulse Response at Various  $T_A$ , Falling Edge,  $A_V = 20$ ,  $V_S = \pm 110$  V,  $V_{OUT} = 200$  V p-p,  $R_F = 100$  k $\Omega$ ,  $R_{LOAD} = 10$  k $\Omega$ ,  $R_{ADJ} = 0$   $\Omega$

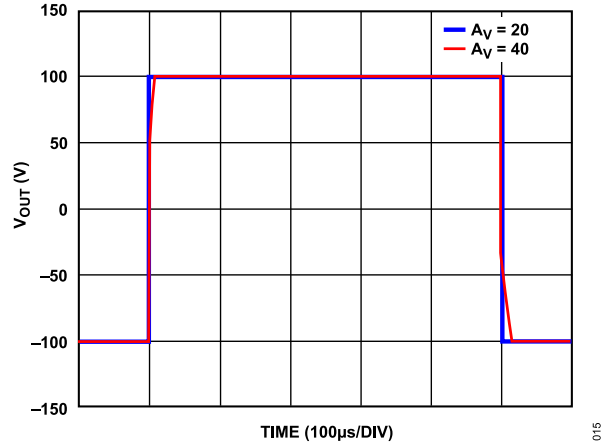


Figure 18. Large Signal Pulse Response at Various Gains,  $T_A = 25^\circ\text{C}$ ,  $V_S = \pm 110$  V,  $V_{OUT} = 200$  V p-p,  $R_F = 100$  k $\Omega$ ,  $R_{LOAD} = 10$  k $\Omega$ ,  $R_{ADJ} = 0$   $\Omega$

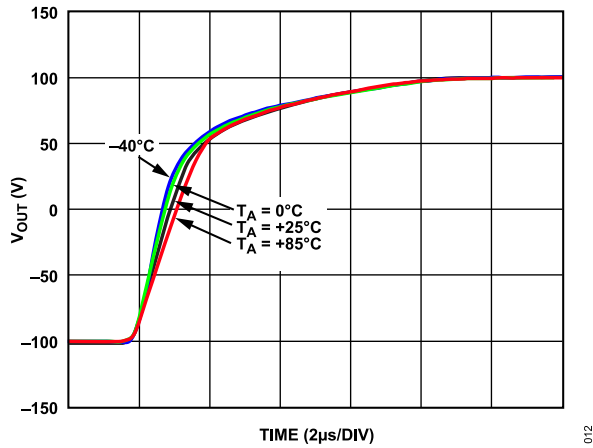


Figure 16. Large Signal Pulse Response at Various  $T_A$ , Rising Edge,  $A_V = 40$ ,  $V_S = \pm 110$  V,  $V_{OUT} = 200$  V p-p,  $R_F = 100$  k $\Omega$ ,  $R_{LOAD} = 10$  k $\Omega$ ,  $R_{ADJ} = 0$   $\Omega$

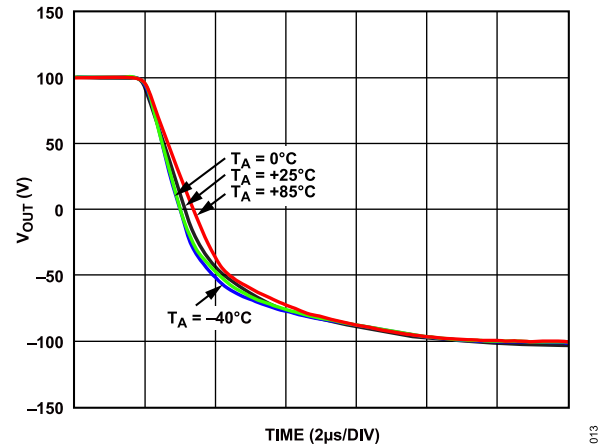


Figure 19. Large Signal Pulse Response at Various  $T_A$ , Falling Edge,  $A_V = 40$ ,  $V_S = \pm 110$  V,  $V_{OUT} = 200$  V p-p,  $R_F = 100$  k $\Omega$ ,  $R_{LOAD} = 10$  k $\Omega$ ,  $R_{ADJ} = 0$   $\Omega$

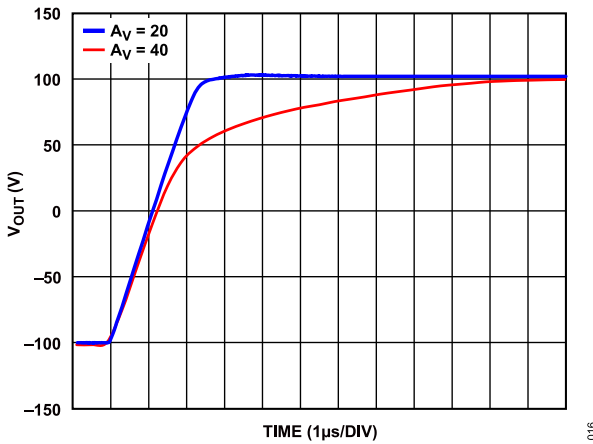


Figure 17. Large Signal Pulse Response at Various Gains, Rising Edge,  $T_A = 25^\circ\text{C}$ ,  $V_S = \pm 110$  V,  $V_{OUT} = 200$  V p-p,  $R_F = 100$  k $\Omega$ ,  $R_{LOAD} = 10$  k $\Omega$ ,  $R_{ADJ} = 0$   $\Omega$

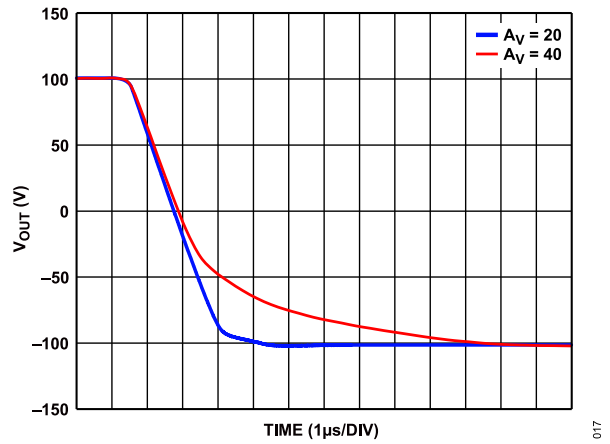


Figure 20. Large Signal Pulse Response at Various Gains, Falling Edge,  $T_A = 25^\circ\text{C}$ ,  $V_S = \pm 110$  V,  $V_{OUT} = 200$  V p-p,  $R_F = 100$  k $\Omega$ ,  $R_{LOAD} = 10$  k $\Omega$ ,  $R_{ADJ} = 0$   $\Omega$

TYPICAL PERFORMANCE CHARACTERISTICS

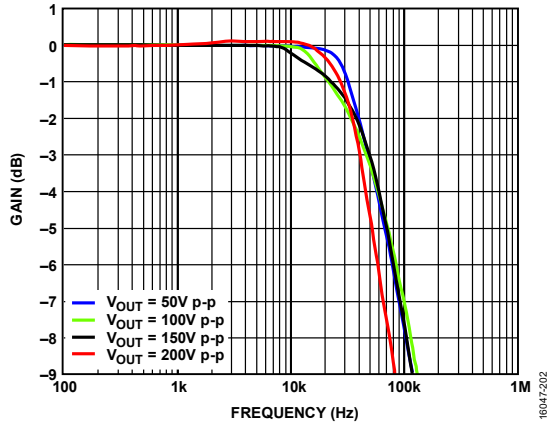


Figure 21. Large Signal Frequency Response at Various Output Swings with Input Clamping Diodes (See the *Slew Boost Circuit and Protection Section*),  $T_A = 25^\circ\text{C}$ ,  $A_V = 40$ ,  $V_S = \pm 110\text{ V}$ ,  $R_F = 100\text{ k}\Omega$ ,  $R_{LOAD} = 10\text{ k}\Omega$ ,  $R_{ADJ} = 0\ \Omega$

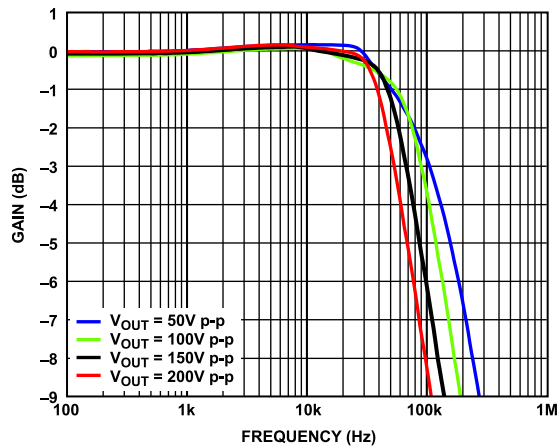


Figure 22. Large Signal Frequency Response at Various Output Swings with Input Clamping Diodes (See the *Slew Boost Circuit and Protection Section*),  $T_A = 25^\circ\text{C}$ ,  $A_V = 20$ ,  $V_S = \pm 110\text{ V}$ ,  $R_F = 100\text{ k}\Omega$ ,  $R_{LOAD} = 10\text{ k}\Omega$ ,  $R_{ADJ} = 0\ \Omega$

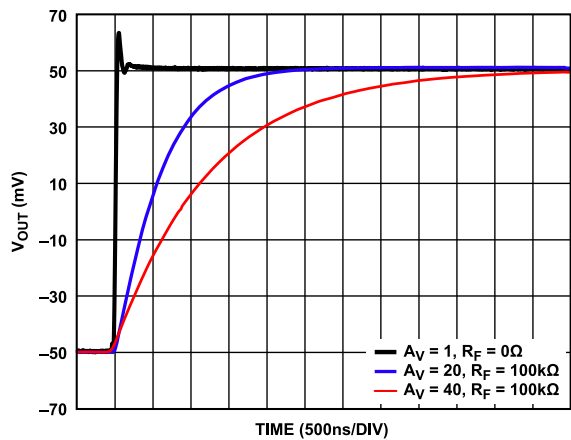


Figure 23. Small Signal Pulse Response at Various Gains, Rising Edge,  $T_A = 25^\circ\text{C}$ ,  $V_S = \pm 110\text{ V}$ ,  $V_{OUT} = 100\text{ mV p-p}$ ,  $R_{LOAD} = 10\text{ k}\Omega$ ,  $R_{ADJ} = 0\ \Omega$

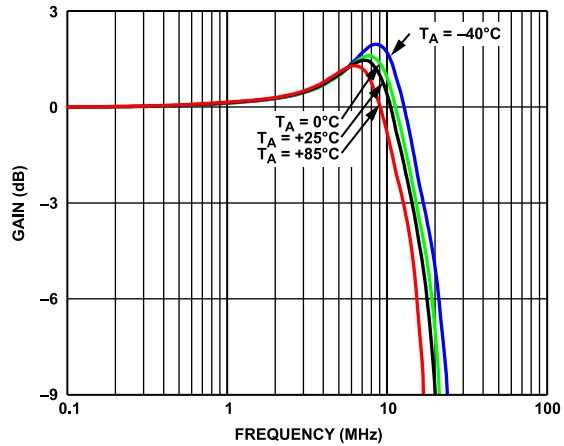


Figure 24. Small Signal Frequency Response at Various  $T_A$ ,  $A_V = 1$ ,  $V_S = \pm 110\text{ V}$ ,  $V_{OUT} = 100\text{ mV p-p}$ ,  $R_L = 10\text{ k}\Omega$ ,  $R_{ADJ} = 0\ \Omega$

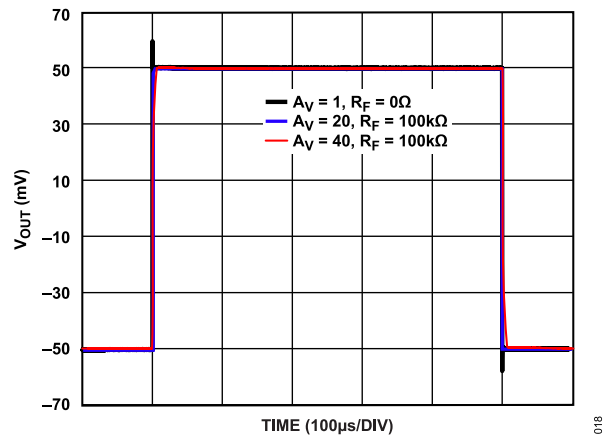


Figure 25. Small Signal Pulse Response at Various Gains,  $T_A = 25^\circ\text{C}$ ,  $V_S = 110\text{ V}$ ,  $V_{OUT} = 100\text{ mV p-p}$ ,  $R_{LOAD} = 10\text{ k}\Omega$ ,  $R_{ADJ} = 0\ \Omega$

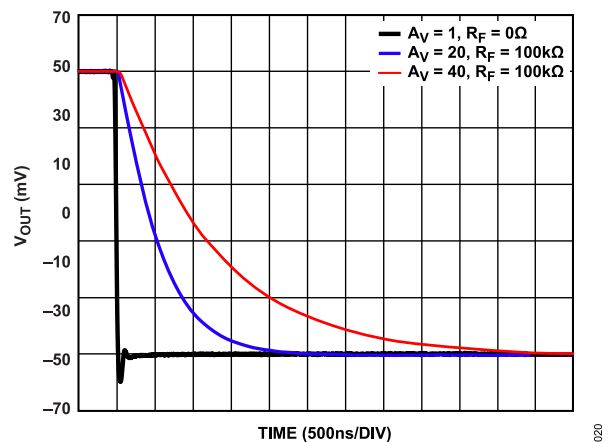


Figure 26. Small Signal Pulse Response at Various Gains, Falling Edge,  $T_A = 25^\circ\text{C}$ ,  $V_S = \pm 110\text{ V}$ ,  $V_{OUT} = 100\text{ mV p-p}$ ,  $R_{LOAD} = 10\text{ k}\Omega$ ,  $R_{ADJ} = 0\ \Omega$

TYPICAL PERFORMANCE CHARACTERISTICS

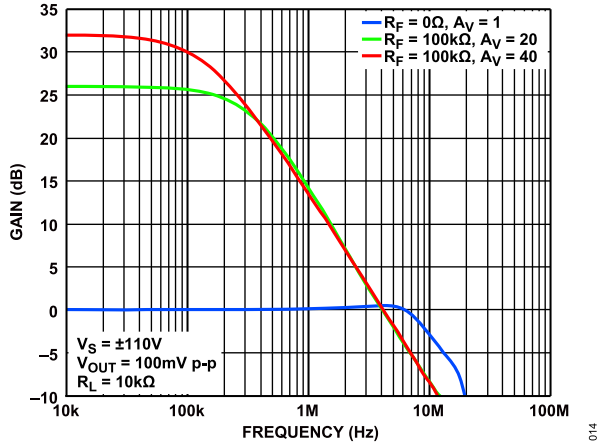


Figure 27. Small Signal Frequency Response at Various Gains,  $T_A = 25^\circ\text{C}$ ,  $V_S = \pm 110\text{ V}$ ,  $V_{OUT} = 100\text{ mV p-p}$ ,  $R_L = 10\text{ k}\Omega$ ,  $R_{ADJ} = 0\ \Omega$

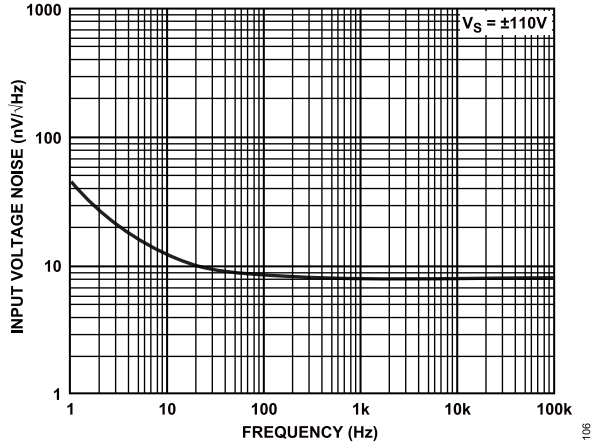


Figure 30. Input Voltage Noise vs. Frequency,  $T_A = 25^\circ\text{C}$ ,  $V_S = \pm 110\text{ V}$ ,  $R_{ADJ} = 0\ \Omega$

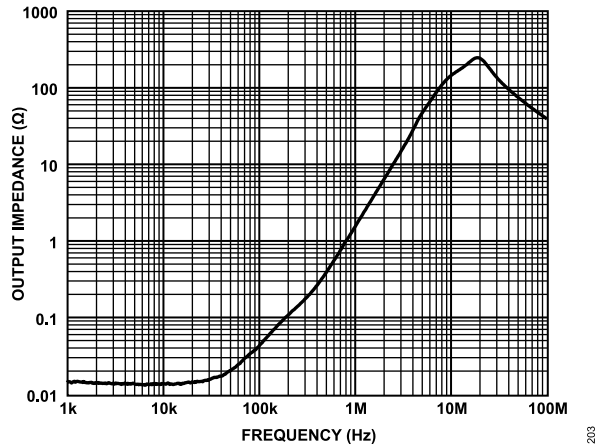


Figure 28. Output Impedance vs. Frequency,  $T_A = 25^\circ\text{C}$ ,  $A_V = 1$ ,  $V_S = \pm 110\text{ V}$ ,  $V_{OUT} = 100\text{ mV p-p}$ ,  $R_F = 0\ \Omega$ ,  $R_{ADJ} = 0\ \Omega$

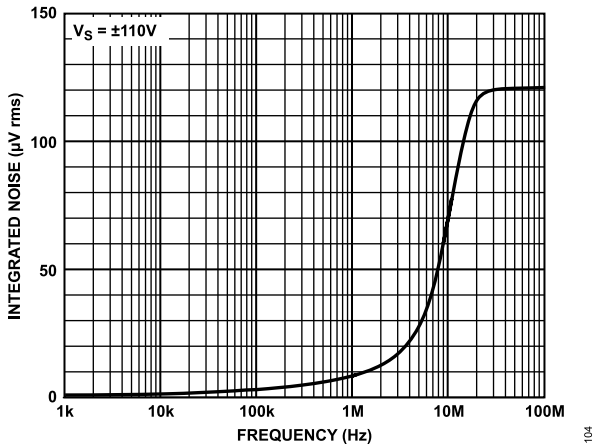


Figure 31. Integrated Noise vs. Frequency,  $T_A = 25^\circ\text{C}$ ,  $V_S = \pm 110\text{ V}$ ,  $R_{ADJ} = 0\ \Omega$

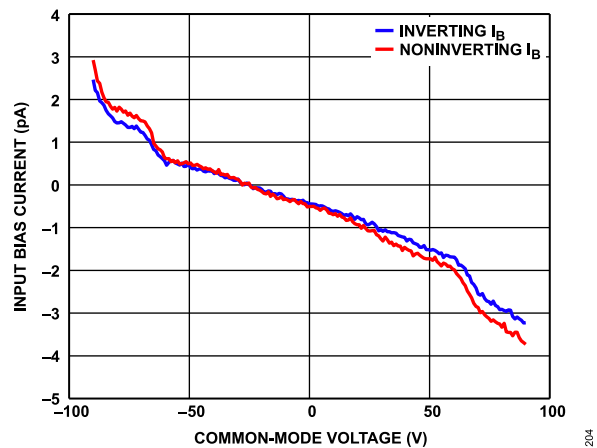


Figure 29. Input Bias Current vs. Common-Mode Voltage,  $T_A = 25^\circ\text{C}$ ,  $V_S = \pm 110\text{ V}$ ,  $R_{ADJ} = 0\ \Omega$

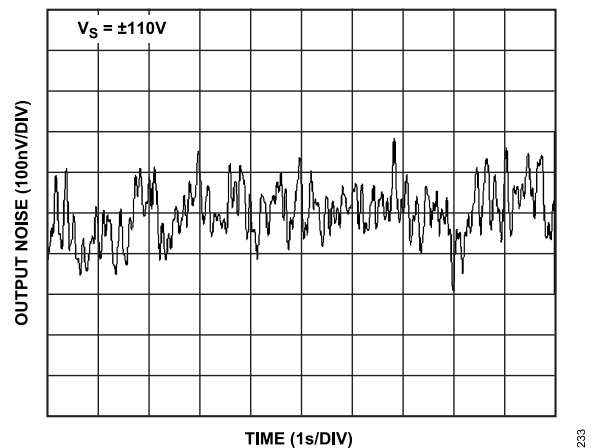


Figure 32. 0.1 Hz to 10 Hz Noise

TYPICAL PERFORMANCE CHARACTERISTICS

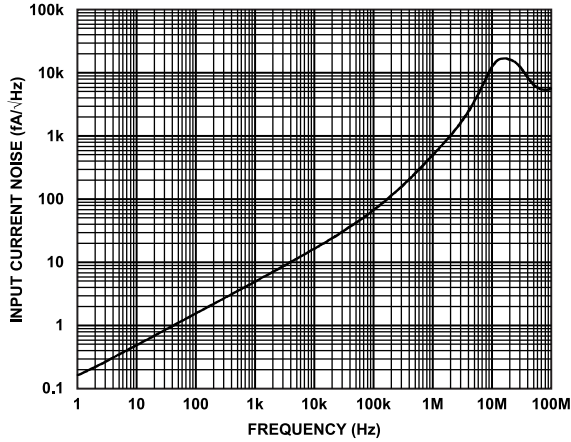


Figure 33. Input Current Noise vs. Frequency

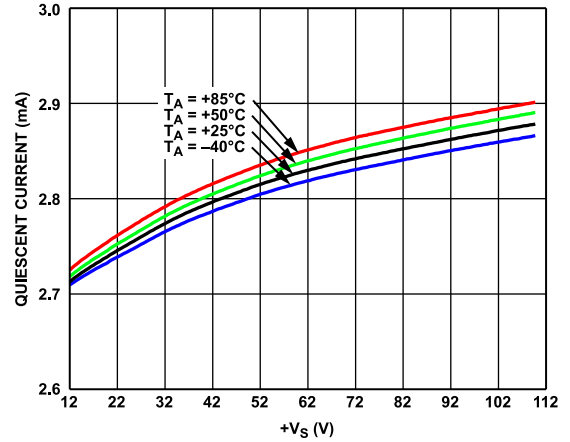


Figure 36. Quiescent Current vs. Positive Supply Voltage at Various  $T_A$ ,  $R_{ADJ} = 0 \Omega$

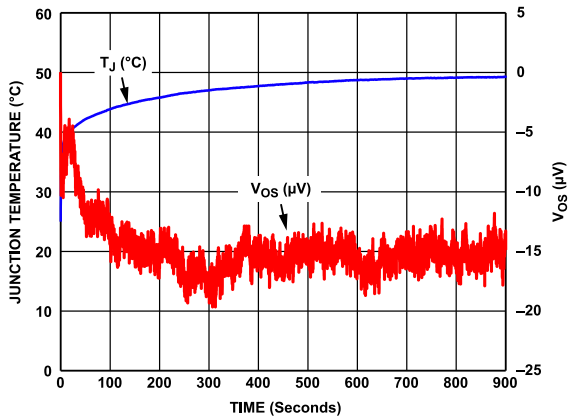


Figure 34. Offset Voltage Warmup Drift and  $T_J$ ,  $V_S = \pm 110$ ,  $R_{ADJ} = 0 \Omega$

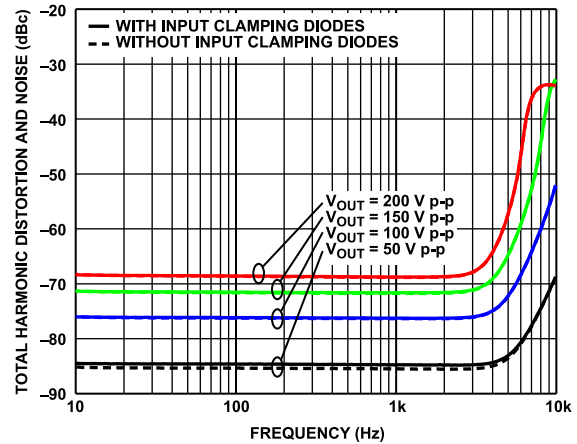


Figure 37. Total Harmonic Distortion and Noise vs. Frequency at Various Large Output Swings,  $T_A = 25^\circ\text{C}$ ,  $A_V = 20$ ,  $V_S = \pm 110 \text{ V}$ ,  $R_F = 100 \text{ k}\Omega$ ,  $R_{LOAD} = 10 \text{ k}\Omega$ ,  $R_{ADJ} = 0 \Omega$

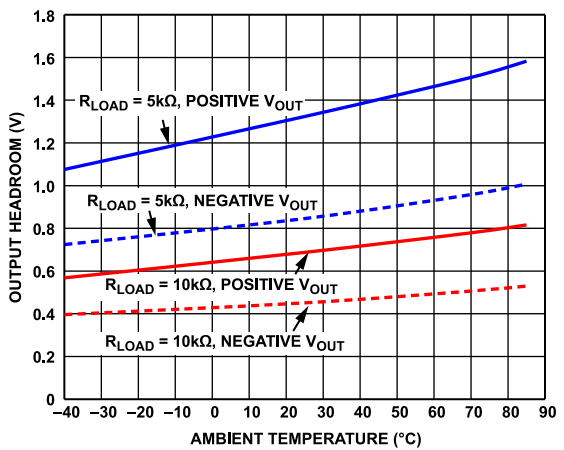


Figure 35. Output Headroom vs. Ambient Temperature at Various  $R_{LOAD}$ ,  $V_S = \pm 110 \text{ V}$ ,  $R_{ADJ} = 0 \Omega$

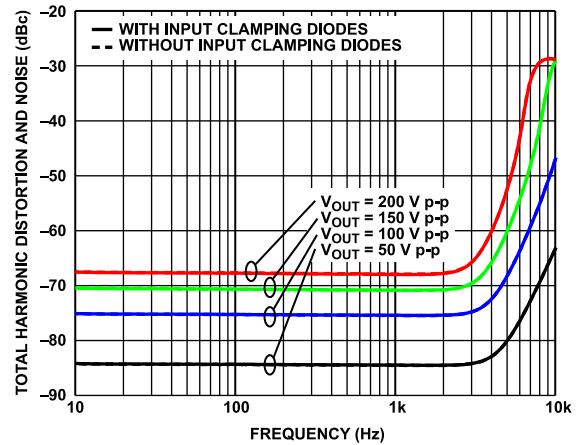


Figure 38. Total Harmonic Distortion and Noise vs. Frequency at Various Large Output Swings,  $T_A = 25^\circ\text{C}$ ,  $A_V = 40$ ,  $V_S = \pm 110 \text{ V}$ ,  $R_F = 100 \text{ k}\Omega$ ,  $R_{LOAD} = 10 \text{ k}\Omega$ ,  $R_{ADJ} = 0 \Omega$

TYPICAL PERFORMANCE CHARACTERISTICS

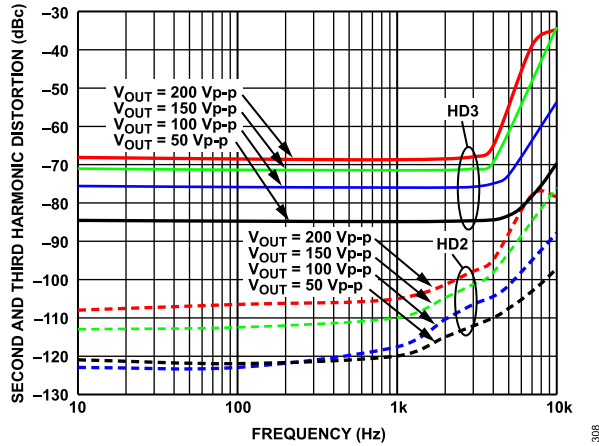


Figure 39. Second Harmonic Distortion (HD2) and Third Harmonic Distortion (HD3) vs. Frequency at Various Output Swings,  $T_A = 25^\circ\text{C}$ ,  $A_V = 20$ ,  $V_S = \pm 110\text{ V}$ ,  $R_F = 100\text{ k}\Omega$ ,  $R_{LOAD} = 10\text{ k}\Omega$ ,  $R_{ADJ} = 0\ \Omega$

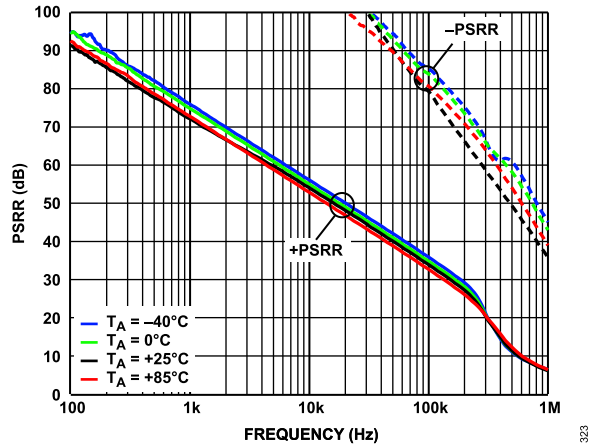


Figure 42. PSRR vs. Frequency at Various  $T_A$ ,  $V_S = \pm 110\text{ V}$ ,  $R_{LOAD} = 10\text{ k}\Omega$ ,  $R_{ADJ} = 0\ \Omega$

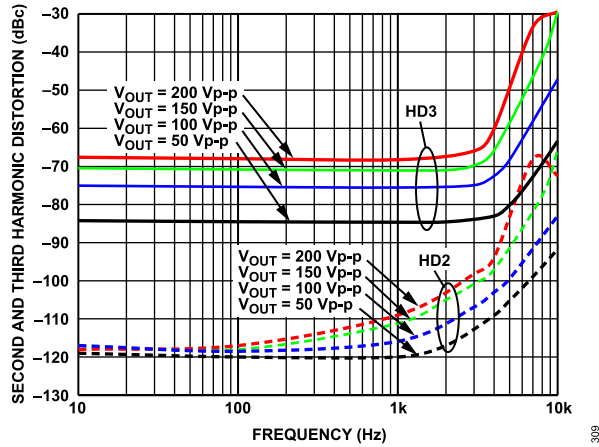


Figure 40. Second Harmonic Distortion (HD2) and Third Harmonic Distortion (HD3) vs. Frequency at Various Output Swings,  $T_A = 25^\circ\text{C}$ ,  $A_V = 40$ ,  $V_S = \pm 110\text{ V}$ ,  $R_F = 100\text{ k}\Omega$ ,  $R_{LOAD} = 10\text{ k}\Omega$ ,  $R_{ADJ} = 0\ \Omega$

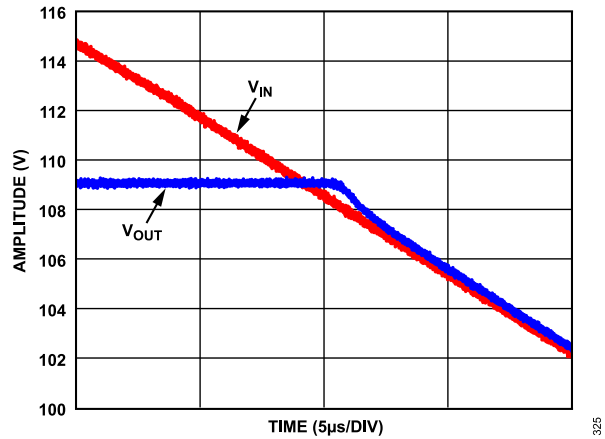


Figure 43. Output Overdrive Recovery,  $V_S = \pm 110\text{ V}$ ,  $A_V = 40$ ,  $R_{LOAD} = 10\text{ k}\Omega$ ,  $R_{ADJ} = 0\ \Omega$

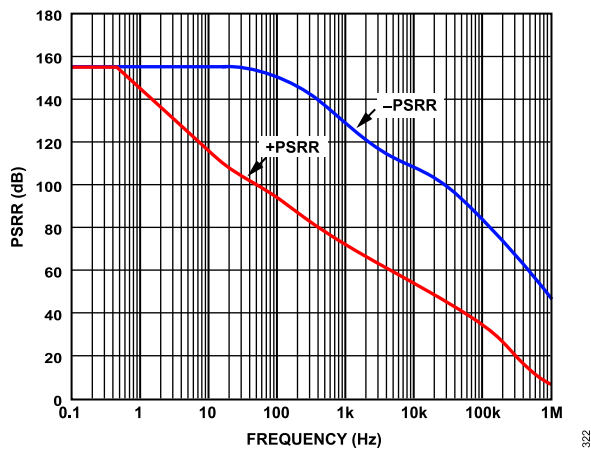


Figure 41. PSRR vs. Frequency,  $T_A = 25^\circ\text{C}$ ,  $V_S = \pm 110\text{ V}$ ,  $R_{LOAD} = 10\text{ k}\Omega$ ,  $R_{ADJ} = 0\ \Omega$

## THEORY OF OPERATION

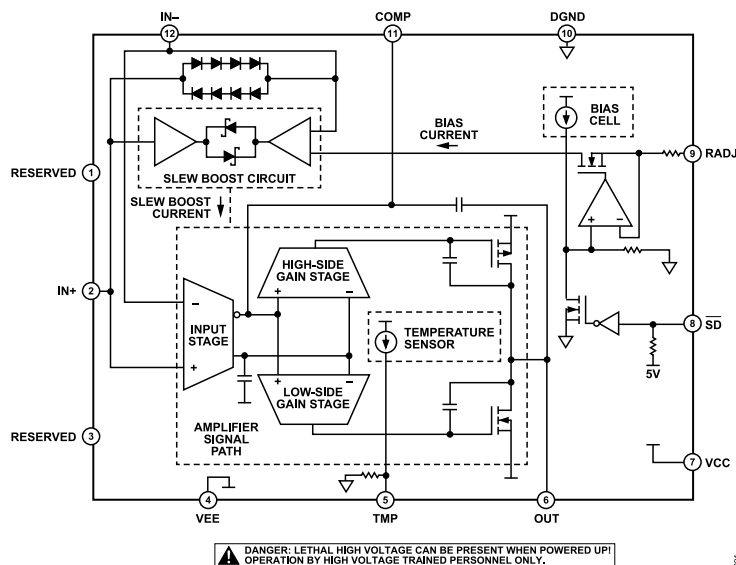


Figure 44. Functional Block Diagram

The ADHV4702-1 is a high voltage (220 V) precision amplifier designed using the next generation of proprietary bipolar/ complementary metal-oxide semiconductor (CMOS)/laterally diffused metal-oxide semiconductor (BCDMOS) process from Analog Devices. Figure 44 shows the functional block diagram. The input stage architecture offers the advantages of high input impedance with low input bias current, low input offset voltage, low drift, and low noise for precision demanding applications, such as automated test equipment (ATE).

## INTERNAL ELECTROSTATIC DISCHARGE (ESD) PROTECTION

As shown in Figure 45, the ADHV4702-1 has an internal ESD configuration to prevent damage due to overvoltage. The ESD protection circuitry involves current steering diodes connected from the input and output pins to the power supply rails. The ADHV4702-1 also includes internal input clamping diodes across the inverting and noninverting inputs to prevent large differential input voltages from damaging the input stage transistors. This input clamping circuit greatly reduces the input impedance for differential input voltages greater than the forward-biased voltage ( $V_F$ ) of four diodes.

The ESD protection circuitry remains inactive under normal operation. To avoid forward biasing the ESD diodes, do not overdrive the pin voltages above the absolute maximum ratings, and ensure that the input differential voltage does not exceed  $4 V_F$ . Additional external input clamping diodes may be required to protect the slew boost circuit. See the [Slew Boost Circuit and Protection](#) section.

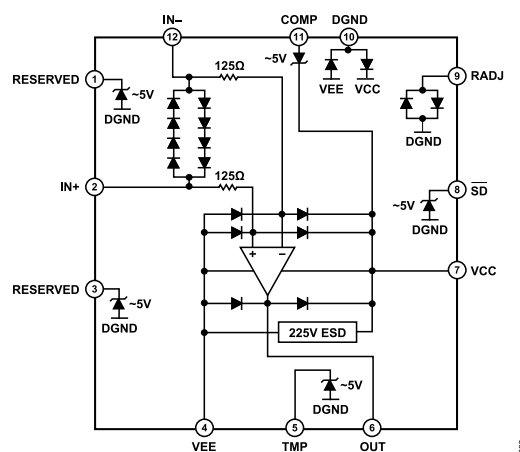


Figure 45. Simplified ESD Configuration

## SLEW BOOST CIRCUIT AND PROTECTION

The ADHV4702-1 uses a supplementary slew boosting circuit to achieve its typical slew rate of  $74 \text{ V}/\mu\text{s}$  across a  $200 \text{ V}$  p-p output range at unity gain. This slew boosting circuit works by sensing the differential input voltage of the amplifier and converting this voltage into a dynamic current to help drive capacitances within the signal path of the amplifier. With greater input voltage across the inputs, more dynamic current is produced, which enables the amplifier to slew faster. The current produced by the slew boosting circuit transmits to all stages of the amplifier during slewing.

Internally, the ADHV4702-1 contains differential input voltage clamps that limit transient differential signals to  $4 V_F$ , placing an upper limit on the slew boost. Large differential input voltages (which can occur with signal frequencies approaching the full power bandwidth) trigger the slew boosting circuit, resulting in an increased dynamic supply current. The relationship between slew rate and full power bandwidth ( $f_M$ ) is given in the following equation:

**THEORY OF OPERATION**

$$SR = V_O \times 2\pi f_M$$

where  $V_O$  is the peak output voltage.

When operating continuously at or near full power bandwidth, the increased supply current may cause an increase in  $T_J$  beyond the safe operating temperature, resulting in device damage. The dynamic safe operating area (SOA) for the EVAL-ADHV4702-1CPZ evaluation board is shown in Figure 61 in the Safe Operating Area section. The dynamic SOA shows the connection between the output swing and the maximum input/output frequency for pulse response. To expand the SOA curve, use additional thermal management or limit the differential voltage across the inputs to  $2 V_F$  with external diodes, which limits the current produced by the slew boosting circuit and reduces the internal power dissipation. Clamping the differential input voltage of the ADHV4702-1 in this way protects the amplifier in dynamic operation but limits slew rate and large signal bandwidth. Figure 46 shows a simplified schematic with external input clamping diodes, and Figure 47 to Figure 50 show the large signal pulse response at various temperatures and gains while the ADHV4702-1 inputs are clamped by two ON Semiconductor SBAV199LT1G diode pairs at  $2 V_F$ .

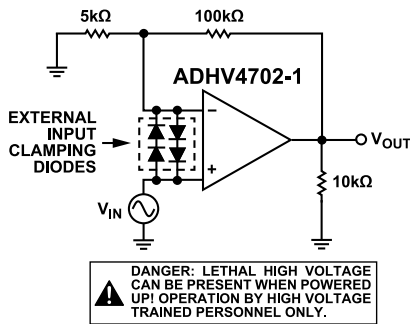


Figure 46. External Input Clamping Diodes Schematic

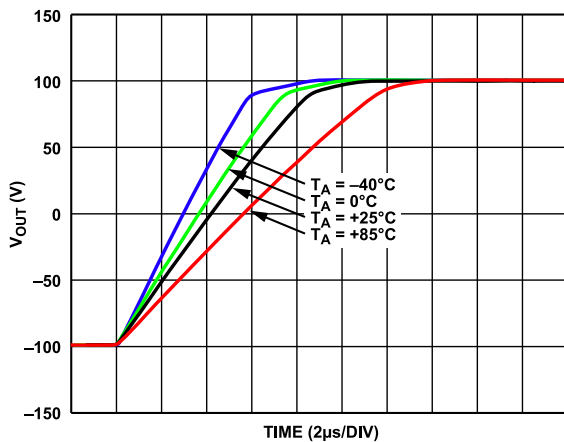


Figure 47. Large Signal Pulse Response at Various  $T_A$  with Two-Diode Forward Voltages, Rising Edge,  $A_V = 20$ ,  $V_S = \pm 110 V$ ,  $V_{OUT} = 200 V$  p-p,  $R_F = 100 k\Omega$ ,  $R_{LOAD} = 10 k\Omega$ ,  $R_{ADJ} = 0 \Omega$

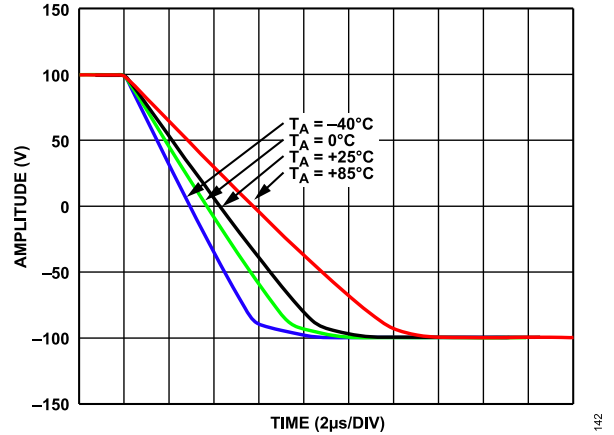


Figure 48. Large Signal Pulse Response at Various  $T_A$  with Two-Diode Forward Voltages, Falling Edge,  $A_V = 20$ ,  $V_S = \pm 110 V$ ,  $V_{OUT} = 200 V$  p-p,  $R_F = 100 k\Omega$ ,  $R_{LOAD} = 10 k\Omega$ ,  $R_{ADJ} = 0 \Omega$

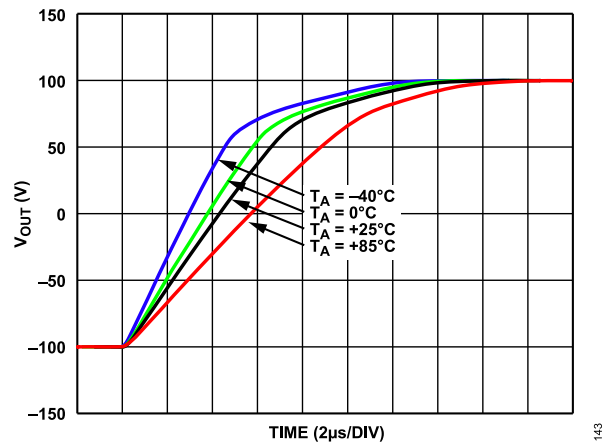


Figure 49. Large Signal Pulse Response at Various  $T_A$  with Two-Diode Forward Voltages, Rising Edge,  $A_V = 40$ ,  $V_S = \pm 110 V$ ,  $V_{OUT} = 200 V$  p-p,  $R_F = 100 k\Omega$ ,  $R_{LOAD} = 10 k\Omega$ ,  $R_{ADJ} = 0 \Omega$

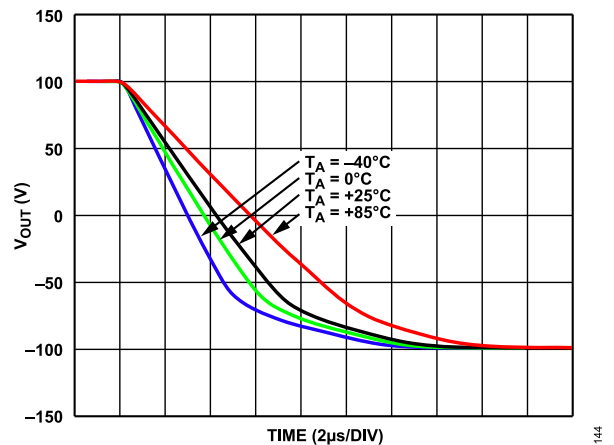


Figure 50. Large Signal Pulse Response at Various  $T_A$  with Two-Diode Forward Voltages, Falling Edge,  $A_V = 40$ ,  $V_S = \pm 110 V$ ,  $V_{OUT} = 200 V$  p-p,  $R_F = 100 k\Omega$ ,  $R_{LOAD} = 10 k\Omega$ ,  $R_{ADJ} = 0 \Omega$



**THEORY OF OPERATION**

**DIGITAL GROUND (DGND)**

DGND is the reference for all low voltage pins of the amplifier (RADJ, TMP, and  $\overline{SD}$ ) and serves as a signal ground for communication to a microprocessor or other low voltage logic circuit. Connect DGND to a 0 V digital ground or analog ground. Do not float DGND.

**RESISTOR ADJUSTABLE QUIESCENT CURRENT (RADJ)**

To reduce further power consumption, the quiescent current of the ADHV4702-1 can be adjusted by placing a resistor ( $R_{ADJ}$ ) between the RADJ pin and DGND.

To fully bias the amplifier, short the RADJ pin directly to DGND to allow maximum dynamic performance. To bias the amplifier with minimum quiescent power consumption, place a 100 k $\Omega$  resistor from RADJ to DGND. This resistor reduces quiescent supply current to approximately 0.6 mA. Operating the amplifier at a lower quiescent current has minimal effect on dc performance but can result in an associated reduction in dynamic performance, such as bandwidth and noise. Figure 51 and Figure 52 show the small signal frequency response and noise performance at various  $R_{ADJ}$  values.

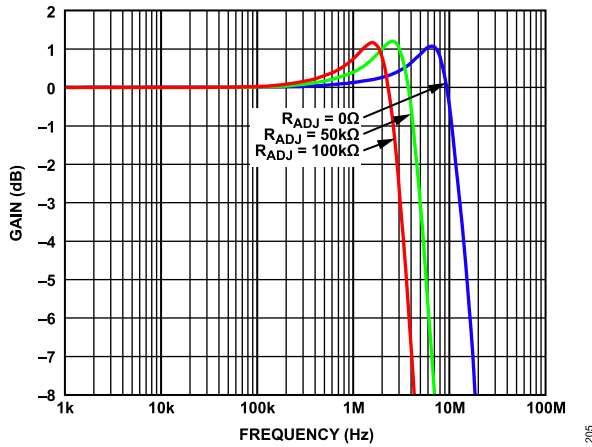


Figure 51. Small Signal Frequency Response at Various  $R_{ADJ}$ ,  $T_A = 25^\circ\text{C}$ ,  $A_V = 1$ ,  $V_S = \pm 110\text{ V}$ ,  $V_{OUT} = 100\text{ mV p-p}$ ,  $R_F = 0\ \Omega$ ,  $R_{LOAD} = 10\text{ k}\Omega$

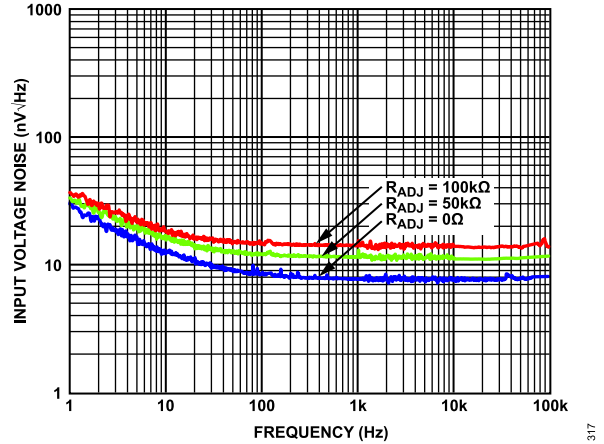


Figure 52. Input Voltage Noise at Various  $R_{ADJ}$ ,  $T_A = 25^\circ\text{C}$ ,  $V_S = \pm 110\text{ V}$

**SHUTDOWN PIN ( $\overline{SD}$ )**

The ADHV4702-1 is equipped with a power saving shutdown feature. When the  $\overline{SD}$  pin voltage is brought low to within 0.8 V of DGND, the amplifier is disabled and put in a low power state, reducing its quiescent current to approximately 0.18 mA. The  $\overline{SD}$  pin has an internal approximately 400 k $\Omega$  pull-up resistor that enables the amplifier if  $\overline{SD}$  is left floating. When turning the amplifier on from the shutdown state, pull the  $\overline{SD}$  pin high to at least 1.6 V above the DGND pin. The  $\overline{SD}$  pin response time for starting up and coming out of shutdown is shown in Figure 53 and Figure 54. The  $\overline{SD}$  pin can support digital logic levels down to 2.5 V. The  $\overline{SD}$  pin can be used to implement thermal shutdown and short-circuit protection when used in conjunction with the temperature monitor feature of the ADHV4702-1.

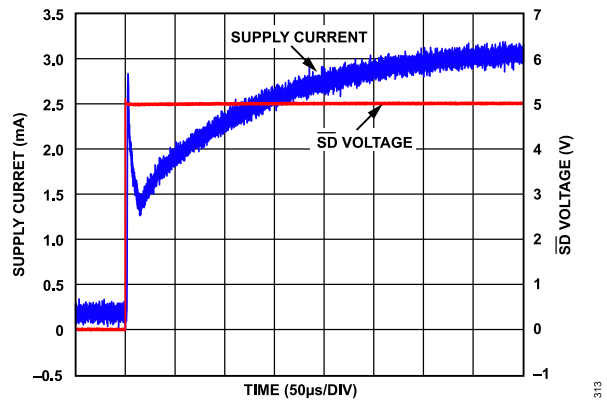
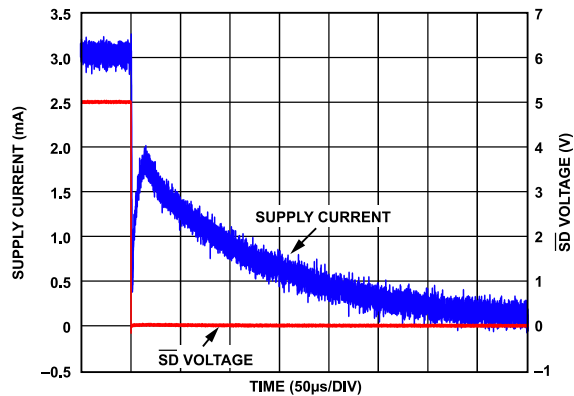


Figure 53.  $\overline{SD}$  Pin Response Time, Turning On



## THEORY OF OPERATION

Figure 54.  $\overline{SD}$  Pin Response Time, Turning Off

## TEMPERATURE MONITOR (TMP)

The ADHV4702-1 features an on-chip temperature sensor in close proximity to the output stage, where die temperature is the highest. The output voltage of the temperature sensor appears at the TMP pin. As an approximate indicator of die temperature, TMP voltage can be used to monitor power dissipation and implement thermal shutdown. The TMP voltage at room temperature is nominally 1.9 V, changing at approximately  $-4.5 \text{ mV}/^\circ\text{C}$ , as shown in Figure 55. More precise temperature readings can be achieved through a one-time room temperature calibration of the TMP pin.

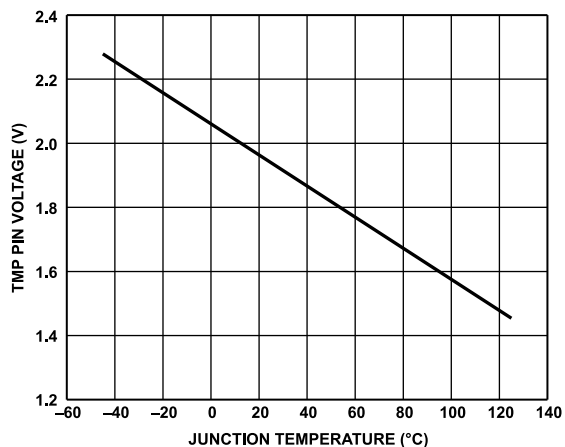


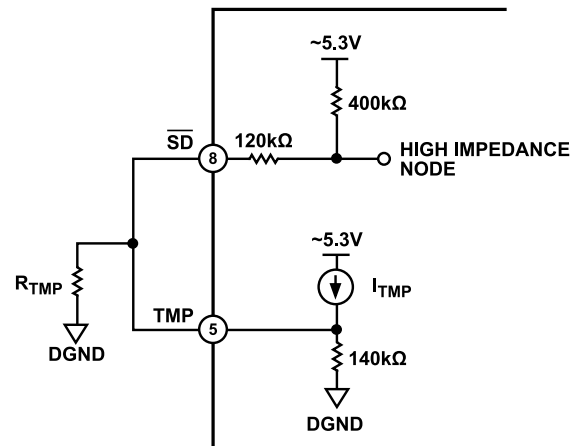
Figure 55. TMP Pin Voltage vs. Junction Temperature

## OVERTEMPERATURE PROTECTION

Operation at or beyond the operating temperature specified in the [Absolute Maximum Ratings](#) section can affect product reliability. To minimize this risk, the ADHV4702-1 features an optional, resistor programmable thermal shutdown where the TMP pin voltage asserts the  $\overline{SD}$  pin. In addition to proper heat sinking, thermal shutdown is recommended to protect the amplifier from an overtemperature condition. To implement the thermal shutdown function, tie TMP to  $\overline{SD}$ , as shown in Figure 56, and connect a  $200 \text{ k}\Omega$  resistor ( $R_{\text{TMP}}$ ) from TMP and  $\overline{SD}$  to DGND in close proximity to the ADHV4702-1.

Device to device variation in the TMP pin voltage may result in different shutdown threshold temperatures or shutdown response times among various devices while implementing the  $200 \text{ k}\Omega$   $R_{\text{TMP}}$ . The shutdown threshold can be adjusted with a smaller  $R_{\text{TMP}}$  resistance, yielding a lower threshold temperature.

The  $R_{\text{TMP}}$  together with the internal resistors of TMP form a voltage divider that influences the TMP pin reading and TMP voltage drift. The TMP data in Table 1 and the [Temperature Monitor \(TMP\)](#) section is only valid when  $R_{\text{TMP}}$  is uninstalled.

Figure 56. TMP and  $\overline{SD}$  Pin Configuration for Short-Circuit Protection and Thermal Shutdown

## OUTPUT CURRENT DRIVE AND SHORT-CIRCUIT PROTECTION

The ADHV4702-1 uses an output stage constructed with cascaded, double diffused, metal-oxide-semiconductor (DMOS) high voltage transistors that provide wide output swing. The ADHV4702-1 can typically drive a  $20 \text{ mA}$  load current continuously. Though with proper thermal management, the ADHV4702-1 can deliver up to  $50 \text{ mA}$ . Short-circuit protection is provided by means of the thermal shutdown feature. To enable short-circuit protection, connect the  $\overline{SD}$  and TMP pins, and tie both to DGND with a  $200 \text{ k}\Omega$   $R_{\text{TMP}}$ .

EXTERNAL COMPENSATION AND CAPACITIVE LOAD ( $C_{\text{LOAD}}$ ) DRIVING

When driving a  $C_{\text{LOAD}}$ , the amplifier output resistance and the load capacitance form a pole in the transfer function of the amplifier. This additional pole reduces phase margin at higher frequencies and, if left uncompensated, can result in excessive peaking and instability. Placing a series resistor ( $R_{\text{S}}$ ) between the amplifier output and  $C_{\text{LOAD}}$  (as shown in Figure 57) allows the ADHV4702-1 to drive capacitive loads beyond  $1 \mu\text{F}$ . Figure 58 shows the series resistor value vs. load capacitance for a maximum of  $2 \text{ dB}$  peaking in the circuit of Figure 57.

In addition to the series resistor, the ADHV4702-1 includes an optional external compensation feature for driving capacitive loads. A capacitor ( $C_{\text{COMP}}$ ) can be installed between COMP and OUT

**THEORY OF OPERATION**

to reduce output stage peaking associated with capacitive loads.  $C_{COMP}$  must be rated for the full supply differential. Figure 60 shows the effect of  $C_{COMP}$  on various capacitive loads.

The values shown in Figure 58, Figure 59, and Figure 60 are for unity gain configuration with a purely  $C_{LOAD}$ . This is a worst case scenario because the amplifier is more stable at higher gains and with some resistive load in parallel with the load capacitance. Although the  $R_S$  or  $C_{COMP}$  significantly increases the stability while driving  $C_{LOAD}$ , they also reduce the headroom and bandwidth while driving a resistive load. For resistive loads, leave the COMP pin floating.

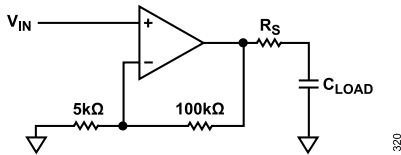


Figure 57. Circuit for  $C_{LOAD}$  Drive

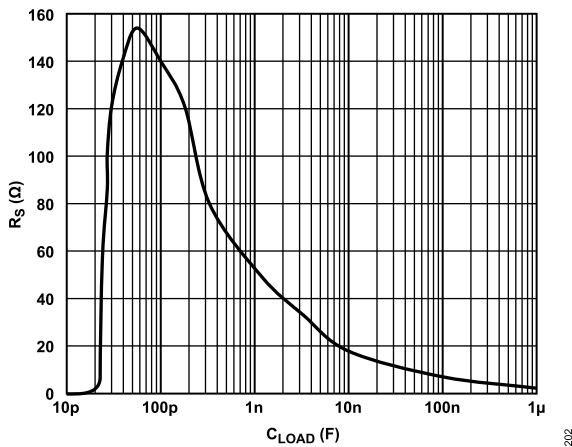


Figure 58.  $R_S$  vs.  $C_{LOAD}$  for Maximum 2 dB Peaking for Circuit from Figure 55,  $T_A = 25^\circ\text{C}$ ,  $A_V = 1$ ,  $V_S = \pm 110\text{ V}$ ,  $V_{OUT} = 100\text{ mV p-p}$ ,  $R_F = 0\ \Omega$ ,  $R_{ADJ} = 0\ \Omega$

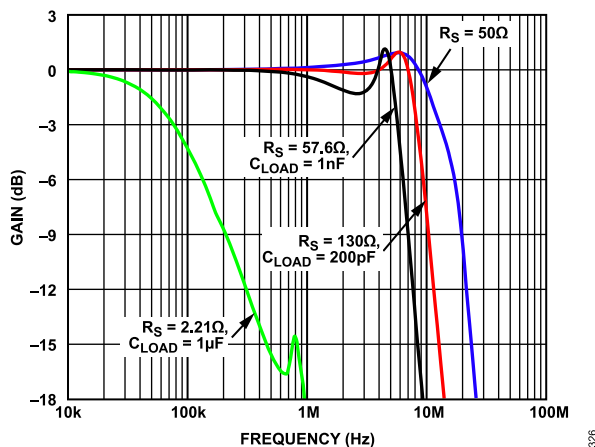


Figure 59. Small Signal Response for Various  $C_{LOAD}$  and  $R_S$  Values,  $T_A = 25^\circ\text{C}$ ,  $A_V = 1$ ,  $V_S = \pm 110\text{ V}$ ,  $V_{OUT} = 100\text{ mV p-p}$ ,  $R_F = 0\ \Omega$ ,  $R_{ADJ} = 0\ \Omega$

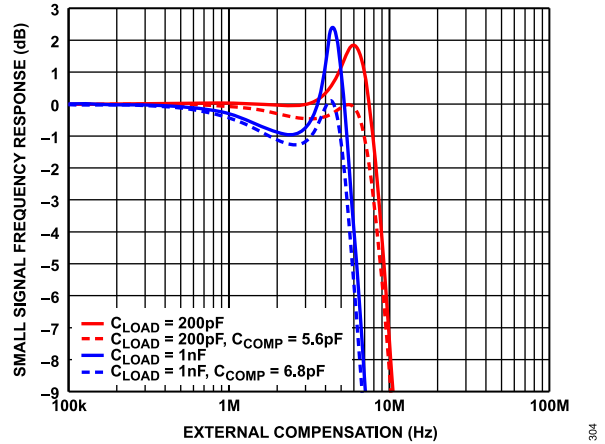


Figure 60. Small Signal Frequency Response vs. External Compensation,  $T_A = 25^\circ\text{C}$ ,  $A_V = 1$ ,  $V_S = \pm 110\text{ V}$ ,  $V_{OUT} = 100\text{ mV p-p}$ ,  $R_F = 0\ \Omega$ ,  $R_{ADJ} = 0\ \Omega$

**SAFE OPERATING AREA**

The SOA represents the power handling capability of the device under various conditions.

The power dissipation of the ADHV4702-1 occurs primarily from the slew boosting circuit and output stage. The slew boosting circuit requires additional supply current. Operating the amplifier at its maximum slew rate at larger swing or at a high frequency increases the current consumption of the slew boosting circuit, increasing the  $T_J$ . Figure 61 shows the dynamic SOA that maintains a  $T_J$  less than  $150^\circ\text{C}$ . The curve shows the maximum safe square wave frequency for a given amplitude. Operating the ADHV4702-1 outside of the boundaries can cause permanent damage. Using additional thermal management or input clamping diodes expands the dynamic SOA significantly. However, using input clamping diodes can compromise the slew rate and the large signal bandwidth.

The dc SOA is a curve of output current vs. the voltage across the output stage, which is the voltage difference between supply and output ( $V_S - V_{OUT}$ ) under which the amplifier can operate at a safe  $T_J$ . The areas under the curves of Figure 62 show the operational boundaries of the ADHV4702-1 that maintain a  $T_J \leq 150^\circ\text{C}$ .

The SOA curves are unique to the conditions under which they were developed, such as PCB, heat sink, and  $T_A$ . All testing was performed in a still air environment. Forced air convection in any of the test cases effectively lowers  $\theta_{JA}$  and expands the SOA.

THEORY OF OPERATION

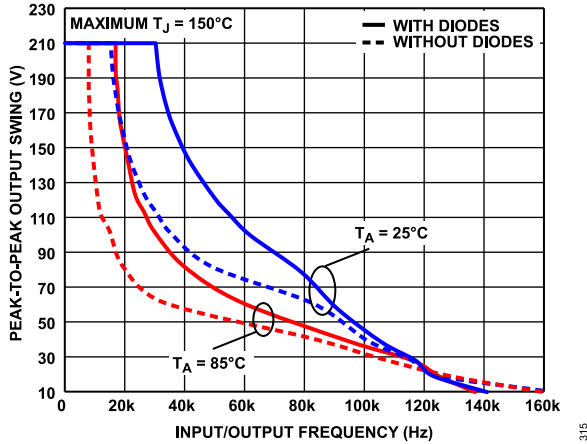


Figure 61. Dynamic SOA at  $T_A = 25^\circ\text{C}$  and  $T_A = 85^\circ\text{C}$  With and Without Input Clamping Diodes,  $A_V = 20$ ,  $V_S = \pm 110\text{ V}$ ,  $R_F = 100\text{ k}\Omega$ ,  $R_{LOAD} = 10\text{ k}\Omega$ ,  $R_{ADJ} = 0\ \Omega$

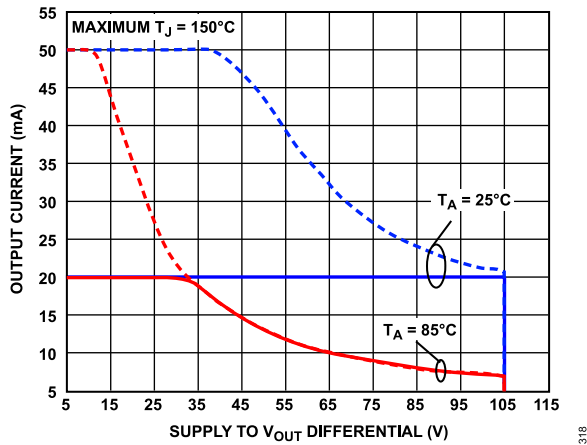


Figure 62. DC SOA at  $T_A = 25^\circ\text{C}$  and  $T_A = 85^\circ\text{C}$ ,  $A_V = 20$ ,  $V_S = \pm 110\text{ V}$ ,  $R_F = 100\text{ k}\Omega$ ,  $R_{ADJ} = 0\ \Omega$

LFCSP PACKAGE AND HIGH VOLTAGE PIN SPACING

A 7 mm × 7 mm, 12-lead LFCSP with EPAD was selected for the ADHV4702-1 to provide high reliability and compliance to regional and global high voltage standards regarding dielectric withstanding (clearance) and carbonization of package surface (creepage). The package dimensions are shown in Figure 66. The ADHV4702-1 meets the minimum 1.25 mm spacing requirement of IEC Standard 61010-1 for creepage distance to preclude failure due to carbon tracking at 250 V rms. To maintain these protections, it is essential to remove all flux and soldering residue around the package pins and exposed pad. Refer to the IEC 61010-1 standard for additional information.

EXPOSED PAD (EPAD)

The copper EPAD of the LFCSP provides a thermally conductive path to the PCB, which can be attached to a heat sink to improve heat dissipation. There is no internal electrical connection to the EPAD. High voltage isolation allows the EPAD to be safely biased to a 0 V ground plane, regardless of VCC or VEE voltages.

APPLICATIONS INFORMATION

POWER SUPPLY AND DECOUPLING

The ADHV4702-1 can operate from a single supply or dual supply. The total supply voltage ( $V_{CC} - V_{EE}$ ) must be between 24 V and 220 V. The ADHV4702-1 requires a minimum supply voltage of  $\pm 12$  V from the reference voltage for normal operation. Decouple each supply pin to ground using high quality, low effective series resistance (ESR), 0.1  $\mu$ F capacitors. Place decoupling capacitors as close to the supply pins as possible. Additionally, place 1.2  $\mu$ F tantalum capacitors from each supply to ground to provide sufficient low frequency decoupling and supply the needed current to support large, fast slewing signals at the ADHV4702-1 output. To ensure reliable operation under high voltages, the voltage ratings for the bypass capacitors must be higher than the supply voltages of the ADHV4702-1.

HIGH VOLTAGE GUARD RING

The ADHV4702-1 features a pin placement that facilitates the use of a guard ring around the noninverting input of the amplifier. Guarding minimizes leakage from nearby pins and helps to achieve the benefit of low input bias current. The guard must be free of solder mask so that it remains exposed on the surface of the PCB. Drive the guard ring to a potential that tracks the input of the amplifier.

HIGH VOLTAGE DAC VOLTAGE SUBTRACTOR

The ADHV4702-1 can be combined with a dual, 16-bit voltage output, DAC, such as the AD5752R, to produce a versatile high voltage DAC solution. For this configuration, set up the ADHV4702-1 as a voltage subtractor with a gain of 20, which is ideally suited for chemical analysis (mass spectrometry), piezodrive, scanning electron microscope (SEM), LiDAR APD/SPAD, and silicon photo-multiplier bias control applications.

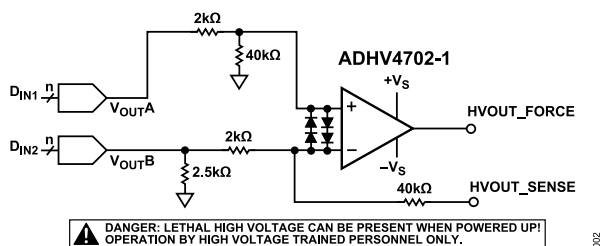


Figure 63. ADHV4702-1 Configured as a Voltage Subtractor Using DACs

HIGH CURRENT OUTPUT DRIVER

Figure 64 shows a system level application of the ADHV4702-1 that boosts the output current drive of the amplifier. By introducing a

discrete unity-gain output stage, the ADHV4702-1 can be used as a high power output driver retaining the precision performance capabilities of the standalone amplifier, such as offset, drift, open-loop gain, and CMRR, while increasing the output current drive up to the current handling capabilities of the discrete devices.

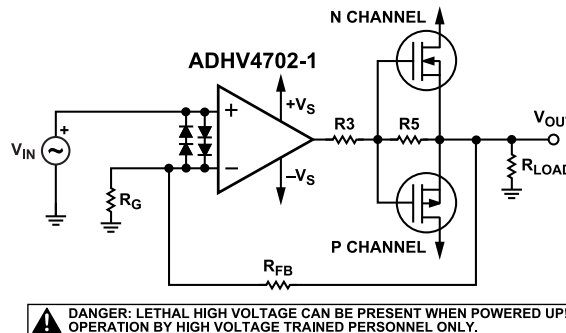


Figure 64. High Current Output Driver Schematic

SIGNAL RANGE EXTENDER

Figure 65 shows an example of a signal range extender configuration. By introducing two additional high power, discrete, metal-oxide semiconductor field effect transistors (MOSFETs), the range extender can deliver at least twice the signal range (depending on the MOSFET selection), while retaining the original performance characteristics of the amplifier.

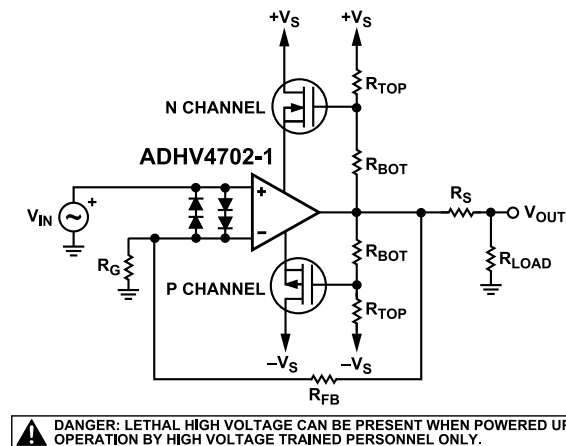


Figure 65. Voltage Extender Schematic